V International Conference on Computational Methods for Coupled Problems in Science and Engineering
COUPLED PROBLEMS 2013
S. Idelsohn, M. Papadrakakis and B. Schrefler (Eds)

# COUPLED SWELLING AND LARGE STRAIN MODEL FOR HYDROGELS: APPLICATION TO THE NUCLEUS PULPOSUS OF THE INTERVERTEBRAL DISC

**V. BRULLIARD*†, S. LE CORRE†† AND E. VERRON†**

*†LUNAM Université, Ecole Centrale de Nantes
GeM-UMR CNRS 6183, 1 rue de la Noé, BP 92101
44321 Nantes, France
e-mail: violette.brulliard@ec-nantes.fr, web page: http://gem.ec-nantes.fr/

††LUNAM Université, Polytech' Nantes
LTN-UMR CNRS 6607, rue Christian Pauc, BP 50906
44306 Nantes, France
e-mail: steven.le-corre@univ-nantes.fr, web page: http://www.polytech.univ-nantes.fr/ltn/fr/

**Key words:** Hydrogel, Coupled Swelling and Large Strain, Intervertebral Disc, Nucleus Pulposus

**Abstract.** *The main constituents of the nucleus pulposus, the central gelatinous part of the intervertebral disc, are water and a solid extracellular matrix of macromolecules. Based on this observation, the nucleus pulposus can be seen as a gel-like material in which swelling - due to the diffusion of the fluid molecules into the macromolecular network - and large strain elasticity, induced by the macromolecular chains, occur. In recent literature, many authors have been interested in describing such a coupled deformation-diffusion problem for gels. Most of the time, these works were formulated with respect to the dry configuration of the material. However, for the nucleus pulposus, the dry configuration does not exist. Thus, the formulation of the deformation-diffusion problem should be modified in order to consider a reference configuration, which is undeformed and unconstrained (but already swollen).*
*The theoretical aspects of the derivation of this coupled deformation-diffusion model is proposed. Then, this model is numerically implemented in the finite element commercial software ABAQUS. The states of equilibrium are investigated on simple homogeneous examples. Finally, the human nucleus pulposus of the intervertebral disc is chosen as a representative complex example of application for this approach. The associated annulus fibrosus is modelled using an anisotropic hyperelastic material law.*

## 1 INTRODUCTION

The role of the intervertebral disc (IVD) is to provide flexibility of the spine, and transmit and distribute large loads through the spine. To carry out these tasks the IVD consists in a particularly complex structure made of a central gelatinous nucleus pulposus (NP) surrounded circumferentially by the annulus fibrosus (AF) as shown in Figure 1. However, due to aging or pathological process, many people show degenerative changes in the IVD, and especially in the NP. These changes affect both its composition and structure, as well as its mechanical functions. Back pain is often a clinical consequence of disc degeneration.

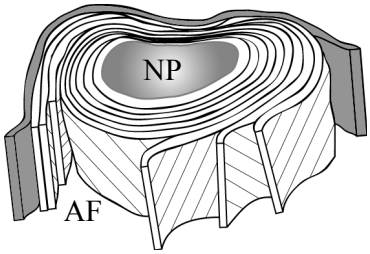


**Figure 1**: Representation of the IVD structure (issued from [1]).

The full understanding of the role of each one of the components of the IVD in the mechanical response of the IVD, as well as the mechanism of disc degeneration, is of major interest. Indeed, it would help proposing solutions to the problem of disc degeneration. In that purpose, finite element models are a very usefull tool. Several finite element models have already been used to predict the behavior of the IVD, to investigate the process of disc degeneration, or to understand the complex exchange mechanisms that occur within the IVD. Anisotropic highly non-linear constitutive models reflecting the physical structure of the AF have been reported [2, 3]. However, relevant constitutive models for the NP are not straightforward. Indeed, for relatively simple purposes, the NP has often been modelled as a non-linear incompressible solid or a fluid [4]. More recently, the NP has been considered as a biphasic material, comprising an incompressible fluid phase that saturates and flows through an elastic isotropic solid phase, leading to complex equations [5]. Our goal is to propose a new approach for modelling the NP. Based on the observation of its constituents - mainly water (about 80 %) and a solid extracellular matrix of structural macromolecules (proteoglycans, collagens) - the NP can be seen as a gel-like system which couples large strain elasticity induced by the macromolecular chains, and swelling properties related to the migration of the solvent throught the network.

In recent literature, some authors have been interested in describing such a coupled deformation-diffusion problem for gels [6, 7, 8]. In most of these works, the problem was formulated with respect to the dry configuration of the material. However, keeping in mind the application to the NP, the derivation of problem should be modified in order to consider a reference configuration which would not be dry, but already swollen (since the

NP initially contains a large quantity of water). To our knowledge, only Lucantonio and coworkers have introduced a reference state which is initially swollen, homogeneous and stress-free, but they do not completely overcome the initial dry configuration [9].

Here, the theoretical aspects of a new constitutive model for gel-like material such as the NP of the IVD, based on an already swollen reference, are developed. This model is then numerically implemented in the finite element commercial software ABAQUS for investigating the states of chemical long-term equilibrium. As benchmark examples, simple homogeneous cases, such as stress-free swelling and uniaxial tension of a cubic sample are studied. Finally, a finite element model of a simplified human intervertebral disc is proposed: the present approach is applied to the central NP, whereas the surrounding annulus fibrosus is classically modelled using an anisotropic hyperelastic material law.

## 2 A CONSTITUTIVE MODEL OF COUPLED SWELLING AND LARGE STRAIN FOR A GEL-LIKE MATERIAL

### 2.1 Kinematics

The gel-like material is considered as single continuum body, subjected to both large strain and solvent diffusion. As usual for the elasticity of soft materials, the general framework of large strain hyperelasticity is adopted, and the material is considered homogeneous and isotropic at the Continuum Mechanics scale.

The reference configuration ($\Omega_0$) of the material body is assumed to be already swollen, undeformed and unconstrained. At time $t > 0$, the body occupies a different region ($\Omega$). The motion of any material point P of position $\mathbf{X}$ in the reference configuration is described by the mapping $\mathbf{x} = \boldsymbol{\varphi}(\mathbf{X}, \mathbf{t})$, where $\mathbf{x}$ denotes the spatial position of P. The deformation gradient is given by $\mathbf{F} = \mathbf{Grad}\boldsymbol{\varphi}$.

A multiplicative decomposition of the deformation gradient $\mathbf{F}$ is adopted:

$$\mathbf{F} = \mathbf{f}\ \mathbf{F_s}, \tag{1}$$

where $\mathbf{F_s}\lambda_s\mathbf{I}$ represents the homogeneous, isotropic deformation due to swelling, from the reference state ($\Omega_0$) to the equilibrium (fully swollen) state ($\Omega_s$), $\lambda_s$ being the equilibrium swelling stretch, and $\mathbf{f}$ stands for the elastic deformation of the gel-like material. Let denote $V_0$ the volume of the material in the reference state, $V_s$ the volume in the swollen state and $V$ the volume in the final state. Thus, we have the following relationship describing the volume changes between the different configurations:

$$J = \det \mathbf{F} = \frac{V}{V_0}, \quad J_s = \det \mathbf{F_s} = \frac{V_s}{V_0}, \quad j = \det \mathbf{f} = \frac{V}{V_s}, \quad \text{and} \quad J = jJ_s. \tag{2}$$

Assuming that both the solid network and the water are incompressible, we have $j = 1$, and $J = J_s$ will describe the swelling degree from the reference configuration.

Assuming that there is no free volume, the volume in the reference configuration $V_0$ and the volume in the swollen configuration $V_s$ are given respectively by:

$$V_0 = V_m + V_{f,0}, \quad \text{and} \quad V_s = V_m + V_f = V_m + V_{f,0} + V_{f,a}, \tag{3}$$

where $V_m$ is the volume of the solid matrix, $V_{f,0}$ the initial volume of fluid, $V_f$ the total volume of the fluid molecules in the swollen state, and $V_{f,a}$ is the volume of fluid molecules added between the reference state and the swollen state. Thus, the swelling degree writes:

$$J_s = \frac{V_m + V_f}{V_m + V_{f,0}} = 1 + \frac{V_{f,a}}{V_0}. \tag{4}$$

Introducing $\nu$ the volume of a fluid molecule, $n_{f,a}$ the number of fluid molecules added between the reference state and the final one, we have

$$J_s = 1 + \frac{\nu n_{f,a}}{V_0} = 1 + \nu c, \tag{5}$$

where $c = n_{f,a}/V_0$ is the number of fluid molecules added per unit of reference volume. Equation (5) is often refered to as the molecular incompressibility constraint [6].

## 2.2 Free energy and constitutive theory

### 2.2.1 General form of the free energy density, thermodynamic restrictions

First, the deformation between $(\Omega_0)$ and $(\Omega_s)$ is due to the diffusion of the fluid molecules in the material. Thus, the Helmholtz free energy which includes the chemical potential of the pure solvent has to be considered, as well as the change in free energy due to mixing of the solvent with the solid network. Secondly, the strain energy between $(\Omega_s)$ and $(\Omega)$ should also be introduced. The total free energy density of the material written per unit reference volume is the sum of these contributions:

$$\Psi(\mathbf{F}) = \Psi(\mathbf{f}, J_s) = \Psi_{\text{pure}}(J_s) + \Psi_{\text{mix}}(J_s) + \Psi_{\text{mech}}(\mathbf{f}, J_s). \tag{6}$$

Considering the general framework of Thermodynamics of Irreversible Processes (see for example [10]) for deformation and diffusion, the Clausius–Duhem inequality issued is:

$$\mathcal{D}_{\text{int}} = \mathbf{P} : \dot{\mathbf{F}} + \mu\dot{c} - \dot{\Psi} - \mathbf{j} \cdot \mathbf{Grad}\mu \geq 0, \tag{7}$$

where $\mathcal{D}_{\text{int}}$ is the internal dissipation, $\mathbf{P}$ is the first Piola-Kirchhoff (nominal) stress tensor, $\mu$ the chemical potential and $\mathbf{j}$ represents the fluid flux. Recalling that $\Psi$ can be written as a function of both the deformation gradient $\mathbf{f}$ and the variable $J_s$, the internal dissipation can be expressed as:

$$\mathcal{D}_{\text{int}} = \mathbf{P} : \dot{\mathbf{F}} + \mu\dot{c} - \left.\frac{\partial \Psi}{\partial \mathbf{f}}\right|_{J_s} : \dot{\mathbf{f}} - \left.\frac{\partial \Psi}{\partial J_s}\right|_{\mathbf{f}} \dot{J}_s - \mathbf{j} \cdot \mathbf{Grad}\mu \geq 0. \tag{8}$$

Deriving the multiplicative decomposition Eq. (1) with respect to time, we have:

$$\dot{\mathbf{F}} = \frac{1}{3} J_s^{-2/3} \dot{J}_s \mathbf{f} + J_s^{1/3} \dot{\mathbf{f}}. \tag{9}$$

Then, using Eq. (9) and the incompressibility constraint Eq. (5) in the second term, Eq. (8) becomes

$$\left( J_s^{1/3} \mathbf{P} - \left. \frac{\partial \Psi}{\partial \mathbf{f}} \right|_{J_s} \right) : \dot{\mathbf{f}} + \left[ \frac{\mu}{\nu} + \frac{1}{3} J_s^{-2/3} \mathbf{P} : \mathbf{f} - \left. \frac{\partial \Psi}{\partial J_s} \right|_{\mathbf{f}} \right] \dot{J}_s - \mathbf{j} \cdot \mathbf{Grad} \mu \geq 0. \tag{10}$$

The next step of the derivation consists in invoking the classical Coleman-Noll procedure.

### 2.2.2 Constitutive equations

The details of the derivation are not given here; only the final constitutive equations are given.

**Stress-strain relationship** Introducing the right Cauchy-Green strain tensor of the purely elastic deformation $\mathbf{c} = \mathbf{f}^T \mathbf{f}$, the first Piola-Kirchhoff stress tensor is

$$\mathbf{P} = -q \mathbf{F}^{-T} + 2 J_s^{-1/3} \mathbf{f} \frac{\partial \Psi_{\text{mech}}}{\partial \mathbf{c}} = -q \mathbf{F}^{-T} + 2 J_s^{-2/3} \mathbf{F} \frac{\partial \Psi_{\text{mech}}}{\partial \mathbf{c}}, \tag{11}$$

where $q$ is an arbitrary scalar (classically reffered to as hydrostatic pressure). Recalling that the Cauchy (true) stress tensor $\boldsymbol{\sigma}$ is related to the first Piola-Kirchhoff stress tensor $\mathbf{P}$ by $\boldsymbol{\sigma} = J_s^{-1} \mathbf{P} \mathbf{F}^T$, we have also

$$\boldsymbol{\sigma} = -q J_s^{-1} \mathbf{I} + J_s^{-1} \frac{\partial \Psi_{\text{mech}}}{\partial \mathbf{c}} \mathbf{f}^T. \tag{12}$$

**Chemical potential-fluid content relationship** The chemical potential is given by

$$\frac{\mu}{\nu} = \left( \frac{d \Psi_{\text{pure}}}{d J_s} + \frac{d \Psi_{\text{mix}}}{d J_s} + \frac{\partial \Psi_{\text{mech}}}{\partial J_s} \right) - \sigma^S, \tag{13}$$

$\sigma^S := \frac{1}{3} \text{tr} \boldsymbol{\sigma} = \frac{1}{3} J_s^{-2/3} \mathbf{P} : \mathbf{f}$ being the isotropic hydrostatic stress.

## 2.3 Specialization of the theory

The very general form of the constitutive equations have been derived. Now, the theory has to be specialized by imposing additional constitutive assumptions on the free energy densities.

Denoting $\mu_0$ the chemical potential of the pure solvent, the free energy density of the pure solvent per unit reference volume is simply:

$$\Psi_{\text{pure}} = \mu_0 c = \frac{\mu_0}{\nu}(J_s - 1). \tag{14}$$

The standard Flory-Huggins free energy [11, 12] for mixing is originally defined per unit dry volume by

$$\Psi_{\text{mix,dry}}(\phi_m) = \frac{kT}{\nu}\frac{1}{\phi_m}\left[(1-\phi_m)\ln(1-\phi_m) + \chi\phi_m(1-\phi_m)\right], \tag{15}$$

where $k$ is the Boltzmann constant, $T$ is the temperature, $\chi$ is a dimensionless parameter denoting the interaction between the fluid and the solid matrix, and $\phi_m = V_m/V$ is the volume fraction of the solid matrix. Equation (15) may be also written in terms of $J_m = 1/\phi_m$:

$$\Psi_{\text{mix,dry}}(J_m) = \frac{kT}{\nu}(J_m - 1)\left[\ln\left(1 - \frac{1}{J_m}\right) + \frac{\chi}{J_m}\right]. \tag{16}$$

Introducing also the relationship $J_m = J_{s,0}J_s$, the free energy density of mixing per unit reference volume becomes:

$$\Psi_{\text{mix}}(J_s) = \frac{1}{J_{s,0}}\Psi_{\text{mix,dry}}(J_m) = \frac{kT}{\nu}\frac{1}{J_{s,0}}(J_{s,0}J_s - 1)\left[\ln\left(1 - \frac{1}{J_{s,0}J_s}\right) + \frac{\chi}{J_{s,0}J_s}\right]. \tag{17}$$

For the deformation of the solid matrix, a simple neo-Hookean formulation is adopted:

$$\Psi_{\text{mech}}(J_s) = \frac{C_0}{2}(I_1 - 3 - 2\ln J_s), \tag{18}$$

$C_0$ being the shear modulus of the material defined per unit reference volume, and $I_1$ being the first invariant of transformation $\mathbf{F}$, related to the first invariant of transformation $\mathbf{f}$ by the relationship $I_1 = \text{tr}\left(\mathbf{F}^T\mathbf{F}\right) = J_s^{2/3} i_1$.

Thus, adding the three contributions given by Eqs. (14), (17), (18), the total free energy density per unit reference volume is:

$$\Psi(\mathbf{f}, J_s) = \frac{\mu_0}{\nu}(J_s - 1) + \frac{kT}{\nu}\frac{1}{J_{s,0}}(J_{s,0}J_s - 1)\left[\ln\left(1 - \frac{1}{J_{s,0}J_s}\right) + \frac{\chi}{J_{s,0}J_s}\right] + \frac{C_0}{2}(I_1 - 3 - 2\ln J_s). \tag{19}$$

Deriving Eqs. (14), (18) and (17) with respect to $J_s$, and Eq. (18) with respect to $\mathbf{c}$, and substituting them into the general expression of the stresses Eqs. (11) and (12) and into the general expression of the chemical potential Eq. (13), the final set of constitutive equations for a gel-like material is:

- Stress

$$\mathbf{P} = -q\mathbf{F}^{-T} + C_0\mathbf{F}, \quad \text{and} \quad \boldsymbol{\sigma} = -qJ_s^{-1}\mathbf{I} + C_0 J_s^{-1}\mathbf{B}, \tag{20}$$

where $\mathbf{B} = \mathbf{F}\mathbf{F}^T$ is the right Cauchy-Green stress tensor of transformation $\mathbf{F}$.

- Chemical potential

$$\frac{\mu-\mu_0}{kT}=\left[\ln\left(1-\frac{1}{J_{s,0}J_s}\right)+\frac{1}{J_{s,0}J_s}+\frac{\chi}{\left(J_{s,0}J_s\right)^2}\right]+\frac{\nu}{kT}J_s^{-1}\left(q-C_0\right). \tag{21}$$

## 3 FINITE ELEMENT IMPLEMENTATION

This constitutive theory for gel-like materials has been implemented into the finite element software ABAQUS, through the user-defined subroutine UHYPER, as proposed in [13]. For that purpose, another form of the free energy density than Eq. (19) has been used, obtained by a Legendre transformation:

$$\hat{\Psi}(\mathbf{f},\mu)=\mu c-\Psi(\mathbf{f},J_s)=\frac{\mu}{\nu}\left(J_s-1\right)-\Psi(\mathbf{f},J_s), \tag{22}$$

keeping in mind the incompressibility constraint Eq. (5). Noting that ABAQUS uses $\bar{I}_1=J_s^{-2/3}I_1$ rather than $I_1$, and normalising the expression by $kT/\nu$, the free energy density expression that has been implemented is the following:

$$\hat{\Psi}_{\mathrm{norm}}(\mathbf{f},\mu)=\frac{\mu-\mu_0}{kT}(J_s-1)-\frac{1}{J_{s,0}}\left(J_{s,0}J_s-1\right)\left[\ln\left(1-\frac{1}{J_{s,0}J_s}\right)+\frac{\chi}{J_{s,0}J_s}\right]$$
$$-\frac{1}{2}\frac{C_0\nu}{kT}\left(J_s^{2/3}\bar{I}_1-3-2\ln J_s\right). \tag{23}$$

The material parameters $C_0$, $\chi$ and $J_{s,0}$ are passed by the user to the subroutine. Practically, rather than $J_{s,0}$, the fluid volume fraction in the reference state defined as $\phi_f=1-1/J_{s,0}$ is used.

To study the equilibrium states, the "normalized" chemical potential variation $(\mu-\mu_0)/kT$ is imposed as a uniform predefined field within the material at each increment; its values is incremented gradually as a loading parameter, from an initial value $(\mu-\mu_0)/kT|_{\mathrm{init}}$ to 0 (corresponding to the chemical equilibrium $\mu=\mu_0$). The initial value should be specified in agreement with the fact that the material is isotropic, and supposed undeformed and unconstrained initially.

## 4 APPLICATIONS

First, two simple homogeneous cases (stress-free swelling and uniaxial tension of a cubic sample) are studied as benchmark examples, in order to emphasize the influence of the reference state. Then, the constitutive approach is applied to the central NP of the IVD. For the different cases, $kT=4\cdot10^{-21}$ J at room temperature, the molecular volume of water is $\nu=3.0\cdot10^{-29}$ m$^3$/molecule, and $\chi=0.1$ is fixed.

## 4.1 Homogeneous examples

### 4.1.1 Free swelling

Cubic samples with different initial fluid content $\phi_f$ are immersed in a fluid bath of chemical potential $\mu_0$ and allowed to swell freely, isotropically, and without constraint. The deformation gradient and the state of stress are simply

$$\mathbf{F} = \lambda_s \mathbf{I}, \quad \text{and} \quad \boldsymbol{\sigma} = \mathbf{0}. \tag{24}$$

Using Eq. (24) together with Eqs. $(20)_2$ and (21) permits to write the equation satisfied by the free-swelling stretch $\lambda_s$:

$$\frac{\mu - \mu_0}{kT} = \left[ \ln\left(1 - \frac{1-\phi_f}{\lambda_s^3}\right) + \frac{1-\phi_f}{\lambda_s^3} + \frac{\chi\,(1-\phi_f)^2}{\lambda_s^6} \right] + \frac{C_0 \nu}{kT}\left(\lambda_s^{-1} - \lambda_s^{-3}\right). \tag{25}$$

Figure 2 shows the free-swelling isotropic stretch $\lambda_s$ as a function of the "normalized" chemical potential variation, for $\phi_f = 30, 60, 80\%$ (the shear modulus in the reference state was taken as $C_0 = 4 \cdot 10^4$ Pa). As expected, the free-swelling stretch $\lambda_s$ increases when one approaches the equilibrium $\mu = \mu_0$, whatever the value of the initial fluid content $\phi_f$. Moreover, as the initial fluid content $\phi_f$ increases, the swelling degree at equilibrium $J_s^e = (\lambda_s^e)^3$ decreases.

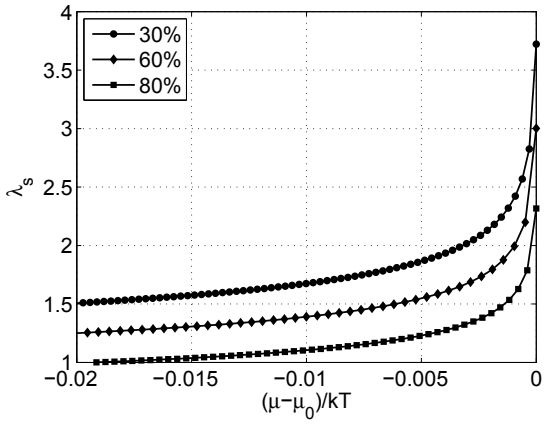


**Figure 2**: Isotropic stretch as a function of the chemical potential for three reference states.

### 4.1.2 Uniaxial tension

Bar sample with different initial fluid content $\phi_f$ are immersed in a fluid bath of chemical potential $\mu_0$ and subjected to uniaxial tension $P_{11}$ in the longitudinal direction $\mathbf{e_1}$. The deformation gradient and the first Piola-Kirchhoff stress tensor are given by:

$$\mathbf{F} = \mathbf{diag}(\lambda_1, \lambda_2, \lambda_2), \quad \text{and} \quad \mathbf{P} = P_{11}\mathbf{e_1}. \tag{26}$$

Substituting Eq. (26) into Eqs. $(20)_1$ and (21) gives the following expressions relating the longitudinal stretch $\lambda_1$, the transverse stretch $\lambda_2$ and the applied load $P_{11}$:

$$\frac{\mu - \mu_0}{kT} = \left[\ln\left(1 - \frac{1-\phi_f}{\lambda_1\lambda_2^2}\right) + \frac{1-\phi_f}{\lambda_1\lambda_2^2} + \frac{\chi\,(1-\phi_f)^2}{\lambda_1^2\lambda_2^4}\right] + \frac{C_0\nu}{kT}\frac{1}{\lambda_1}\left(1 - \frac{1}{\lambda_2^2}\right), \tag{27}$$

and

$$P_{11} = C_0\left(\lambda_1 - \frac{\lambda_2^2}{\lambda_1}\right). \tag{28}$$

The equilibrium is attained when $\mu = \mu_0$. Figure 3 compares the transverse stretch $\lambda_2$ and the "normalized" nominal stress $P_{11}$ for imposed longitudinal stretch $\lambda_1$ for various initial fluid volume fraction in the reference state $\phi_f = 30, 60, 80\%$, at $C_0 = 4{\cdot}10^4$ Pa. Figure 3 (left) shows that the transverse stretch $\lambda_2$ is smaller as the value of the initial fluid content $\phi_f$ gets greater. The isotropic stretch at swelling equilibrium $\lambda_s^e$ for each reference state is obtained at the intersection with the dotted curve: we have $\lambda_s^e = 3.7, 3.0, 2.3$ for $\phi_f = 30, 60, 80\%$ respectively. This is consistent with the previous observations regarding the free-swelling case. Figure 3 (right) shows the traction/compression behaviour of the different materials *from the swollen state* $\lambda_1/\lambda_s^e$. When the initial fluid content $\phi_f$ increases, the longitudinal stress is smaller. Indeed, the material gets softer as the fluid contents gets higher.

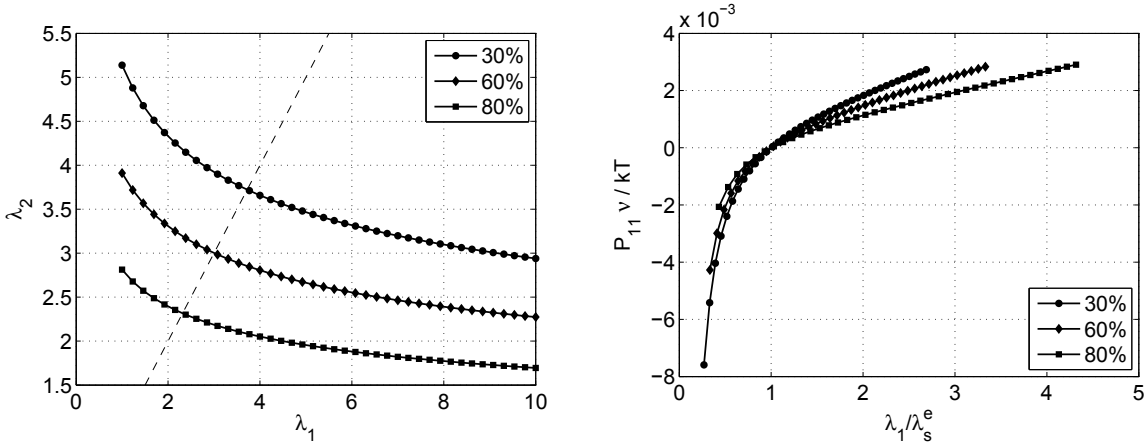


**Figure 3**: Transverse stretch (left) and "normalized" nominal stress (right) versus longitudinal stretch for three reference states.

### 4.2 Simplified human intervertebral disc

The human IVD consists in three main structures: a central cavity filled by the gelatinous NP, a surrounding AF, and the cartilaginous endplates that sandwich the whole. The finite element (FE) model is based on a simplified geometry: the NP and the AF are considered as coaxial cylinders. The radius of the NP is set to 10 mm, the radius of the total IVD is set to 20 mm, the height of the AF and the NP is set to 12mm, and the thickness of the endplates are 1 mm. Due to the numerous symmetries of the problem, only $1/8^{\text{th}}$ of the geometry can be modelled. The endplate, much stiffer than the AF and the NP, are considered as rigid bodies. The NP is modelled using the gel-like model developed here, while the AF is modelled using a anisotropic hyperelastic Holzapfel strain energy potential, proposed in [14] and available in ABAQUS. The material parameters applied for the simulations are listed in Table 1. The inner NP and the outer AF are assumed to be tied together, as well as the top NP and AF faces with the endplate. As loading conditions, an uniaxial displacement of 1 mm is applied on the top endplate.

**Table 1**: Material parameters ([a] see [2])

| | | | | | |
|---|---|---|---|---|---|
| AF | ground substance | $C_{10} = 0.05$ MPa | $D = 0$ | | |
| | fibers | $k_1 = 3$ MPa [a] | $k_2 = 10$ [a] | $\kappa = 0$ | $\gamma = \pm 30°$ |
| NP | | $C_0 = 0.1$ MPa | $\chi = 0.1$ | $\phi_f = 80\%$ | |

Figure 4 shows the mechanical response of the IVD. The order of magnitude of the FE results is consistent with the experimental data issued from [15].

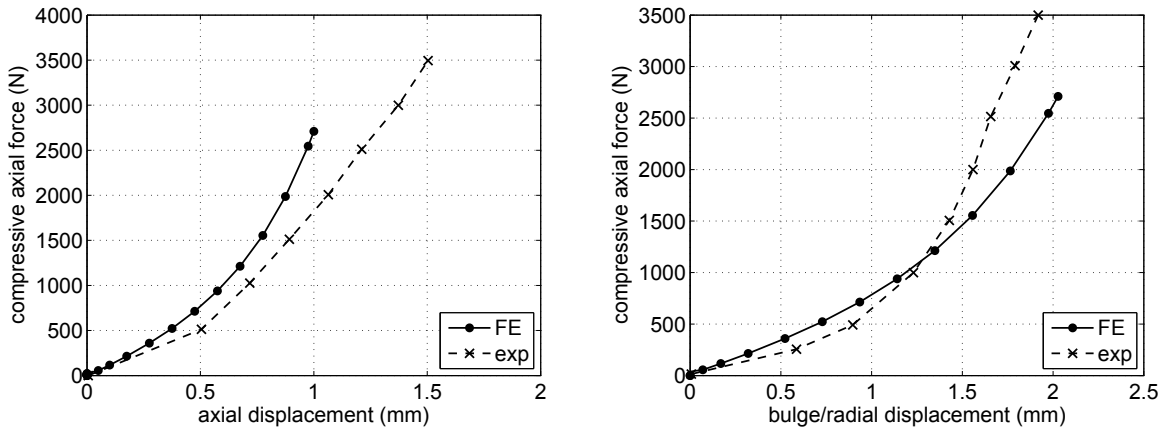


**Figure 4**: Axial compressive force versus axial displacement (left) and radial displacement (right).

It should be noted that for this model, several assumptions were made; among them: (i) the geometry was considered cylindrical while the IVD has more a bean-like shape;

(ii) the AF material parameters were considered constant and uniform, while, as shown in [2, 16], the fibers orientation angle as well as the AF material parameters $k_1$ and $k_2$ strongly depend on the anatomical IVD region; (iii) the contacts between the different disc components were considered tied, which is probably not the case in reality. Taking into account all these realistic features is currently in progress.

## 5 CONCLUSIONS

In the present paper, a theoretical constitutive model for gel-like materials has been derived. The originality of this approach lies in the fact that the reference configuration is already swollen, undeformed and unconstrained. The model has been implemented in a finite element software, and successfully tested on simple homogeneous examples. Finally, the human nucleus pulposus was chosen as a complex example of application of this approach. Early simulations of a simplified intervertebral disc under compressive load show good promises regarding the prediction of the mechanical response of a healthy disc as compared as experimental data. As future work, it is believed that this model could be used to model disc degeneration through appropriate kinetik laws describing the change in stiffness and the fluid loss due to ageing.

## REFERENCES

[1] Campana, S. *Evaluation of the relationship between biomechanical properties and imaging: an in vitro study of the intervertebral disc.* PhD Thesis in French. Ecole Nationale Supérieure d'Arts et Métiers de Paris (2004).

[2] Eberlein, R., Holzapfel, G.A. and Schulze-Bauer, C.A.J. An anisotropic model for annulus tissue and enhanced finite element analyses of intact lumbar disc bodies. *Comput. Methods Biomech. Biomed. Eng.* (2001) **4**:209–229.

[3] Peng, X.Q., Guo, Z.Y. and Moran, B. An anisotropic hyperelastic constitutive model with fiber-matrix shear interaction for the human annulus fibrosus. *J. Appl. Mech.* (2006) **73**:815–824.

[4] Meakin J.R. and Hukins, W.L. Replacing the nucleus pulposus of the intervertebral disk: prediction of suitable properties of a replacement material using finite element analysis. *J. Mater. Sci. - Mater. Med.* (2001) **12**:207–213.

[5] Ehlers, W., Karajan, N. and Markert, B. An extended biphasic model for charged hydrated tissues with application to the intervertebral disc. *Biomech. Model. Mechanobiol.* (2009) **8**:233—251.

[6] Hong, R., Zhao, X., Zhou, J. and Suo, Z. A theory of coupled diffusion and large deformation in polymeric gels. *J. Mech. Phys. Solids* (2008) **56**:1779–1793.

[7] Chester, S.A. and Anand, L. A coupled theory of fluid permeation and large deformations for elastomeric materials. *J. Mech. Phys. Solids* (2010) **58**:1879–1906.

[8] Duda, F.P., Souza, A.C. and Fried, E. A theory for species migration in a finitely strained solid with application to polymer network swelling. *J. Mech. Phys. Solids* (2010) **58**:515–529.

[9] Lucantonio, A., Nardinocchi, P. and Teresi, L. Transient analysis of swelling-induced large deformations in polymer gels. *J. Mech. Phys. Solids* (2013) **61**:205–218.

[10] Maugin, G.A. and Taylor, R.L. *The Thermodynamics of Nonlinear Irreversible Behaviors: an Introduction.* World scientific series on nonlinear science, Vol. 27 of series A, (1999).

[11] Flory, P.J. Thermodynamics of high polymer solutions. *J. Chem. Phys. Solids* (1942) **10**:51–61.

[12] Huggins, M.L. Some properties of solutions of long-chain coumpounds. *J. Phys. Chem.* (1942) **46**:151–158.

[13] Hong W., Liu, Z. and Suo Z. Inhomogeneous swelling of a gel in equilibrium with a solvent and mechanical load. *Int. J. Solids Struct.* (2009) **46**:3282–3289.

[14] Gasser, T.C., Ogden, R.W. and Holzapfel, G.A. Hyperelastic modelling of arterial layers with distributed collagen fibre orientations. *J. R. Soc. Interface* (2006) **3**:15–35.

[15] Brown, T., Hansen, R.J. and Yorra, A.J. Some mechanical tests on the lumbosacral spine with particular reference to intervertebral discs. *J. Bone Joint Surg.* (1957) **39**:1135–1164.

[16] Holzapfel, G.A, Schulze-Bauer, C.A.J., Feigl, G. and Regitnig, P. Single lamellar mechanics of the human lumbar anulus fibrosus. *Biomechan. Model. Mechanobiol.* (2005) **3**:125–140.